JOURNAL OF GEOPHYSICAL RESEARCH, VOL. 114, E00E07, doi:10.1029/2009JE003417, 2009

Ground ice at the Phoenix Landing Site: Stability state and origin

Michael T. Mellon,[1] Raymond E. Arvidson,[2] Hanna G. Sizemore,[1] Mindi L. Searls,[1] Diana L. Blaney,[3] Selby Cull,[2] Michael H. Hecht,[3] Tabatha L. Heet,[2] H. Uwe Keller,[4] Mark T. Lemmon,[5] Wojciech J. Markiewicz,[4] Douglas W. Ming,[6] Richard V. Morris,[6] W. Thomas Pike,[7] and Aaron P. Zent[8]

Received 1 May 2009; revised 11 August 2009; accepted 2 September 2009; published 17 December 2009.

[1] A primary objective of the Phoenix mission was to examine the characteristics of high latitude ground ice on Mars. We report observations of ground ice, its depth distribution and stability characteristics, and examine its origins and history. High latitude ground ice was explored through a dozen trench complexes and landing thruster pits, over a range of polygon morphological provinces. Shallow ground ice was found to be abundant under a layer of relatively loose ice-free soil with a mean depth of 4.6 cm, which varied by more than 10x from trench to trench. These variations can be attributed mainly to slope effects and thermal inertia variations in the overburden soil affecting ground temperatures. The presence of ice at this depth is consistent with vapor-diffusive equilibrium with respect to a mean atmospheric water content of 3.4×10^{19} m^{-3}, consistent with the present-day climate. Significant ice heterogeneity was observed, with two major forms: ice-cemented soil and relatively pure light toned ice. Ice-cemented soils, which comprised about 90% of the icy material exposed by trenching, are best explained as vapor deposited pore ice in a matrix supported porous soil. Light toned ice deposits represent a minority of the subsurface and are thought to consist of relatively thin near surface deposits. The origin of these relatively pure ice deposits appears most consistent with the formation of excess ice by soil ice segregation, such as would occur by thin film migration and the formation of ice lenses, needle ice, or similar ice structures.

Citation: Mellon, M. T., et al. (2009), Ground ice at the Phoenix Landing Site: Stability state and origin, *J. Geophys. Res.*, *114*, E00E07, doi:10.1029/2009JE003417.

1. Introduction

[2] The distribution and dynamics of water in its various forms is a central focus in the study of Mars. Ground ice, subsurface ice in any concentration, in the Martian permafrost is an integral component of the overall inventory of water and plays a dynamic role in the Martian climatic and geologic history. This ice can exchange with the atmosphere and polar caps, have a pronounced influence on the geomorphic character of the landscape, provide water for geochemical processes and potential for biological processes, and it can trap organic and inorganic molecules of interest for long periods at depths and locations where ground ice remains sedentary.

[3] One of the primary objectives of the Mars Scout mission Phoenix, was to explore the occurrence, characteristics, and distribution of ground ice at a high latitude location, to better understand its role in the Martian environment. To this end, the Phoenix spacecraft landed in a high latitude region dominated by polygonally patterned ground, believed to form as a result of the influences of ground ice, and in a region broadly characterized as containing abundant subsurface hydrogen, based on results from the Mars Odyssey spacecraft [*Smith et al.*, 2008, 2009].

[4] Prior to the Phoenix mission, our understanding of the state, distribution, and dynamics of ground ice has been based on inferences from data returned by various orbiters, and from theoretical studies of water thermophysics and stability. *Leighton and Murray* [1966] initially predicted that ice would be stable at these high latitudes and a suite of theoretical analyses have since examined various aspects of this prediction, from seasonal changes in ice stability [*Farmer and Doms*, 1979; *Paige*, 1992] to the dynamic

[1]Laboratory for Atmospheric and Space Physics, University of Colorado at Boulder, Boulder, Colorado, USA.
[2]Department of Earth and Planetary Sciences, Washington University, Saint Louis, Missouri, USA.
[3]Jet Propulsion Laboratory, Pasadena, California, USA.
[4]Max Planck Institute für Sonnensystemforschung, Katlenburg-Lindau, Germany.
[5]Department of Atmospheric Science, Texas A&M University, College Station, Texas, USA.
[6]NASA Johnson Space Center, Houston, Texas, USA.
[7]Electrical and Electronic Engineering, Imperial College of London, London, UK.
[8]NASA Ames Research Center, Moffett Field, California, USA.

0148-0227/09/2009JE003417$09.00

response of ground ice to long-term climate change [*Fanale et al.*, 1986; *Mellon and Jakosky*, 1995; *Chamberlain and Boynton*, 2007; *Zent*, 2008], the geographic variability in the distribution of ice [*Paige*, 1992; *Mellon and Jakosky*, 1993], and the effects of factors such as soil properties, surface slopes, and rocks [*Kossacki and Markiewicz*, 2002; *Kossacki et al.*, 2003; *Aharonson and Schorghofer*, 2006; *Sizemore and Mellon*, 2006]. Some key findings of these studies were that (1) atmospheric water vapor will readily diffuse into the soil and condense as ice in the pore space; (2) ice is stable at an abrupt boundary (the ice table) below which ice rich material will persist and above which dry, ice-free soil will occur; and (3) within the upper meter of permafrost the ground ice is dynamic, coming and going with obliquity and other orbital cycles. Water ice is currently not stable at the Martian surface, except in the polar regions well north of the Phoenix landing site or shaded areas such as crater interiors. Observational evidence of ground ice has come in two forms. First, images reveal geologic landforms that are believed to form in ice-rich permafrost. The most pervasive of these landforms is polygonal patterned ground. Second, is the detection of hydrogen in the Martian subsurface by the Mars Odyssey spacecraft, which has been explained as subsurface water in high concentrations [e.g., *Boynton et al.*, 2008; *Feldman et al.*, 2008].

[5] The purpose of this paper is to present the first direct in situ observations of ground ice in the Martian northern plains as represented at the Phoenix landing site. Through analysis of these observations and the complex heterogeneity that has been revealed, a better understanding of the context and history of ground ice can emerge. In this work, we also examine the ground ice in terms of its stability with respect to the Martian climate, the Phoenix landing site representing the Northern Plains of Mars, and the possible origin and history of the ice.

2. Phoenix Observations

[6] The Phoenix spacecraft touched down on the Martian northern plains at 68.219° N areocentric latitude and 234.249° E longitude in a relatively flat and level region dominated by polygonally patterned ground, represented by regularly distributed low mounds and a network of perimeter troughs [*Mellon et al.*, 2008b, 2009]. These topographic patterns are generally caused by active thermal contraction cracking in ice-rich permafrost. The troughs (a couple decimeters deep) are zones of gradual consumption of surface fines into subsurface cracks in the ice-rich permafrost, and the mounds are zones of uplift. Deformation and differential heaving of the surface and subsurface allows examination of each of these zones for differences in pedologic and hydrologic histories.

[7] During its 152 sol mission the Phoenix team, using the robot arm (RA) and scoop, excavated 12 trench complexes into about 1/3 the soil surface of the $\sim$3 m^2 work space north to northeast of the lander, exposing various deposits of ice-rich material at the ice table beneath a layer of relatively dry and weakly cohesive soil [*Arvidson et al.*, 2009]. A variety of mechanical, spectral, and chemical analyses showed that these exposures were composed of water ice and soil mixtures in various concentrations [*Smith et al.*, 2009; *Arvidson et al.*, 2009; *Blaney et al.*, 2009; *Boynton et al.*, 2009; *Morris et al.*, 2008]. The trenches were distributed over a range of polygon provinces including the top and side of the interior mounds, and the troughs and trough shoulders. Surface Stereo Imager (SSI) data [*Smith et al.*, 2008] allowed for detailed topographic analysis of both pretrenching and posttrenching surfaces.

[8] Figure 1 shows a map of the RA work space indicating the location of trenches, named rocks, and polygon morphology. Trenched exposures of ice are varied in physical characteristics as well as depths below the original soil surface. An initial trench, Dodo, later merged with the trench Goldilocks, exposed a patch of light toned ice (Figure 2). Additional trenches Upper Cupboard and Ice Man revealed more light toned ice. Small fragments of this ice broke free during trenching, showing the ice was at least partially friable unlike other icy exposures, and sublimated in a few sols leaving no discernable residue [*Smith et al.*, 2009], indicating a high ice concentration. Subsequent monitoring showed the exposed icy surface recessed as it darkened by formation of a sublimation lag [*Morris et al.*, 2008; *Blaney et al.*, 2009], which along with photometric analysis indicated a soil content of no more than 1–2% [*Arvidson et al.*, 2009] of sandy-silt sized particles [*Pike et al.*, 2008]. The light toned nature (Lambert albedo of approximately 0.5) suggests a high degree of scattering of visible light which could be accomplished by gas-filled pores between crystal interfaces within the ice, consistent with its structural weakness. The extent of the light toned ice is limited to the trenches in the northwest portion of the work space, accounting for about 10% of the icy exposures excavated by the RA.

[9] Other excavated exposures of ground ice exhibited characteristics akin to ice-cement soil. In the trenches Snow White, Burn Alive, Neverland, Pet Donkey and LaMancha, digging encountered extensive hard ice-cemented material (see Figure 2). This ground ice was evidenced by RA motion impedance, the formation of chatter marks as the RA dug across the icy surface [*Arvidson et al.*, 2009; *Bonitz et al.*, 2008], and exposure of small (few mm size) patches of darker and bluish material that faded over time [*Blaney et al.*, 2009; *Morris et al.*, 2008]. Additional digging and scraping of these surfaces in Snow White and Burn Alive also exposed larger (several cm size) dark toned patches (Figure 2d) that brightened over time to a tone comparable to the surrounding soil as the ice exposed to sunlight sublimated [*Morris et al.*, 2008; *Blaney et al.*, 2009]. These surfaces could then be scraped further to remove the loose soil lag and expose a fresh hard, icy surface [*Arvidson et al.*, 2009]. The absence of a measurable recession of the icy surface during sublimation indicated that the ground ice exhibited a high soil content, such as in the case of ice filling the pores of a preexisting soil [*Morris et al.*, 2008]. Drilling the ground ice in Snow White with the RA rasp tool generated motor current consistent with ice-cemented soils with about 45% ice by volume [*Arvidson et al.*, 2009]. Additionally, extensive digging and scraping with the RA's titanium blade did little to excavate into the icy surface nor break off fragments of icy material. Together with the dark toned nature, indicating an absence of light scattering gas pores within the ice, these observations suggested the soil was nearly to fully pore saturated with ice.

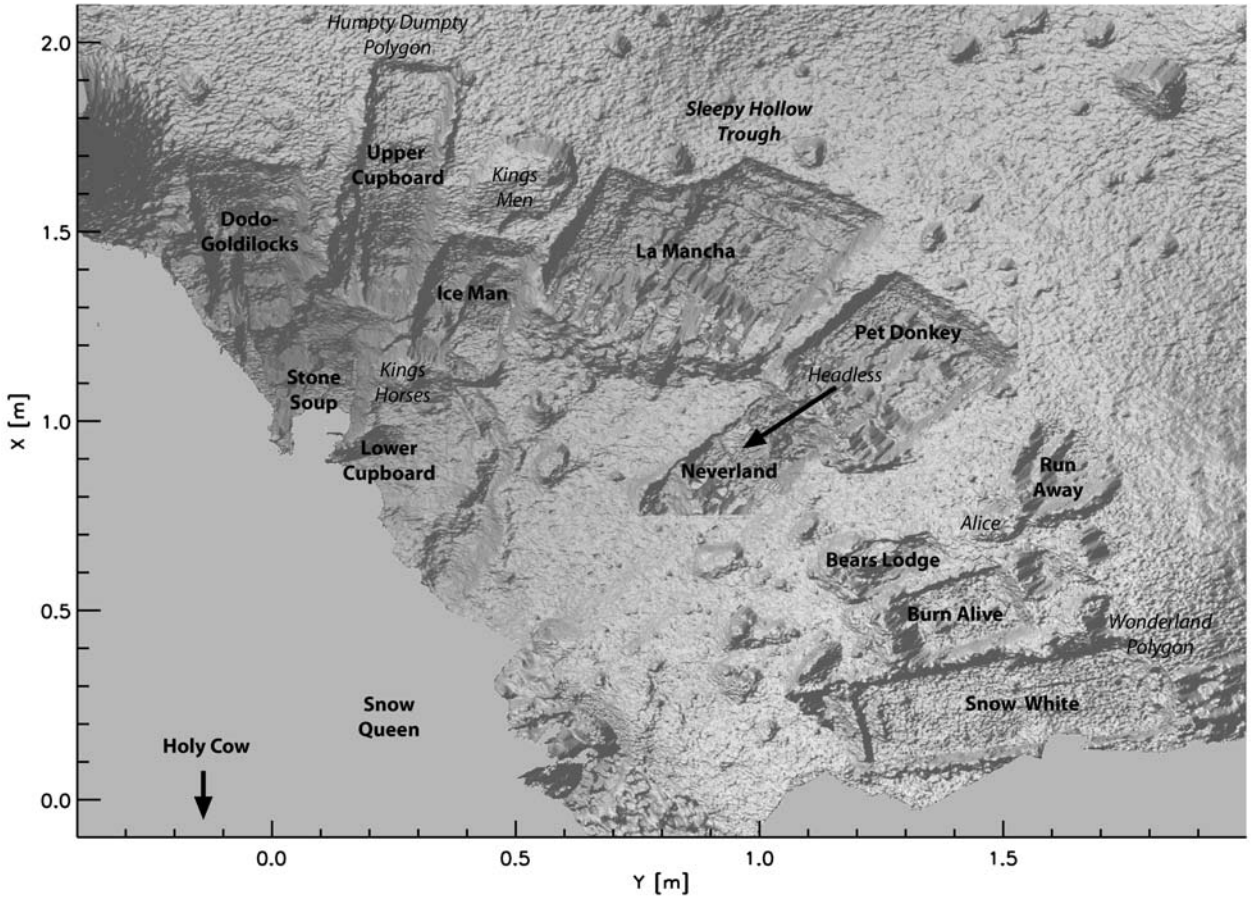

Figure 1. Map of the Phoenix work space showing named trench complexes and thruster pits, including major rocks and polygon features (italics). The coordinate system is relative to the spacecraft payload frame. North is in the direction of the $+x$ axis.

[10] In about 1/3 of the excavated areas the RA did not encounter strong evidence of ground ice. Operational considerations limited digging further into these areas, due to the limited mission timeline or considerations of the RA proximity to the lander deck. While the RA may have dug to ice or just above the ice, these trenches did not offer clear evidence of an ice table surface (e.g., no chatter marks, no visible ice, nor motion impedance that could not be easily attributed to a subsurface rock). It is expected that the ice-rich permafrost in the landing site region is continuous based on stability thermophysics [e.g., *Mellon et al.*, 2004; *Aharonson and Schorghofer*, 2006]. Trenching results and analysis do not offer evidence to suggest otherwise.

[11] In addition to excavation of the surface by the RA, the 12 thrusters used to control the landing process stripped loose soil from the ice table under the lander, revealing a ring of flat-floored near-circular pits each about 50 cm in diameter. Two pairs of pits shown in Figure 3, named Holy Cow near the southern (−X) footpad and Snow Queen near the eastern (+Y) footpad were imaged by the robotic arm camera (RAC) [*Keller et al.*, 2009]. A third pair was not fully imaged. These surfaces are perhaps the cleanest exposures of the ice table achieved by Phoenix, though potentially altered by the brief (∼1s or less) pulsed impingement of hydrazine decomposition products as the loose soil was cleared away during landing [*Mehta et al.*, 2008].

[12] The floor of the thruster pits exhibited a soil like tone and texture, which may result from imbedded soil, residual loose fines, or a combination. Holy Cow (Figure 3a) appears brighter in patches than Snow Queen (Figures 3b and 3c) which may be due to either lighter toned ice or the high phase angle of direct solar illumination on smooth ice-saturated soil. Also shown in Figure 3b are four impingement points from the thrusters final pulses onto the surface of the Snow Queen pit. These points appeared brighter which may be due to clearing residual fines from a smooth ice-saturated soil surface, exposure of brighter ice, or refreezing of a thin melt layer. The surfaces of both Holy Cow and Snow Queen undulate slightly on the centimeter scale, but lack large variations except a rock pit in Snow Queen [*Sizemore et al.*, 2009] and possible polygon thermal contraction cracks [*Mellon et al.*, 2009]. Ice-cemented soil textures are clearly visible in the closer images of Snow Queen (Figure 3c). These spatially varying textures at or near the fracture zone in a polygon trough indicate a complex history of soil grains incorporated into a growing sand wedge [*Mellon et al.*, 2009].

[13] The thruster pits were monitored throughout the mission for change detection, as exposed water ice is not stable in the current climate. These surfaces were observed

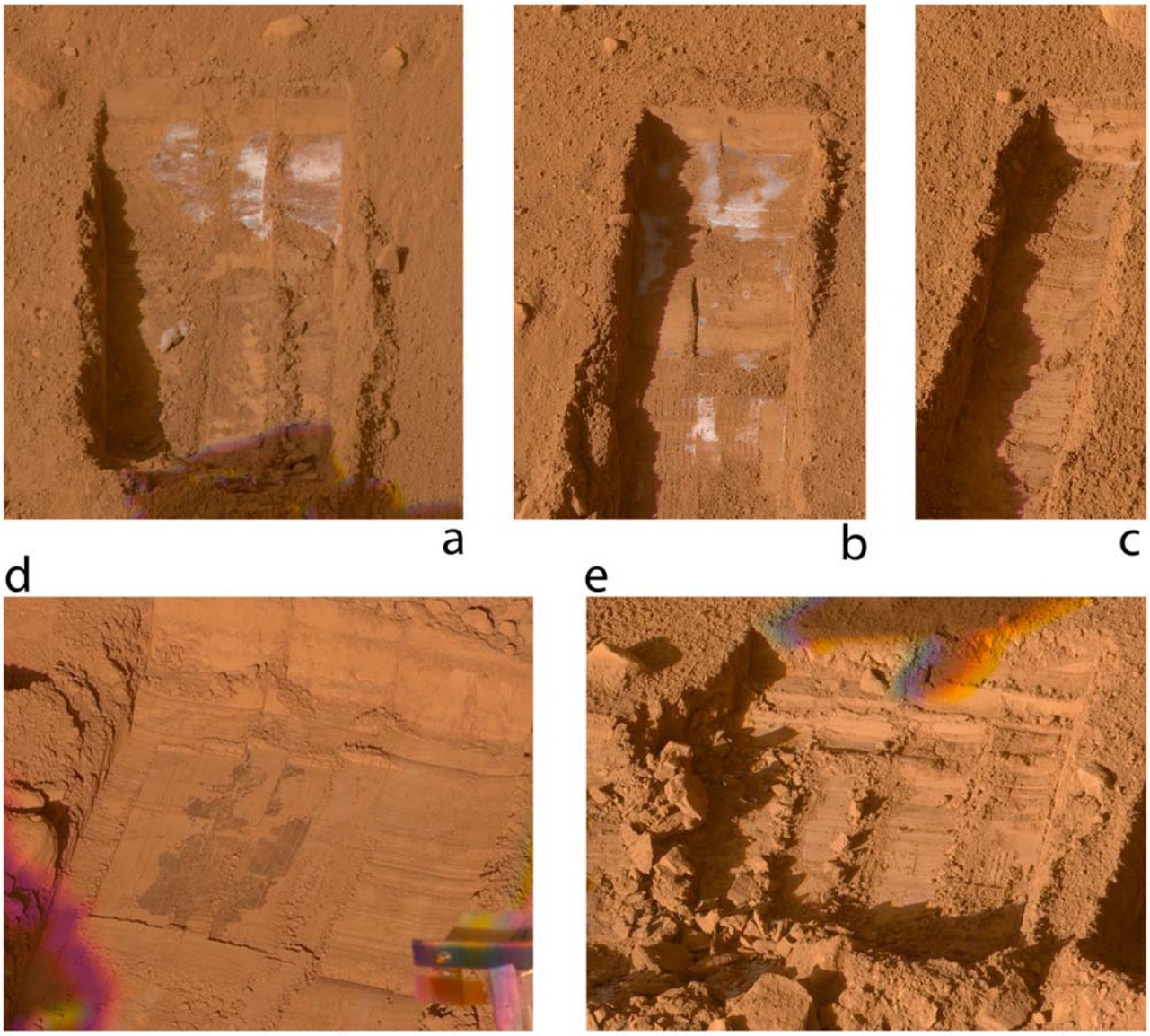

Figure 2. Examples of icy material exposed during trenching. Light toned ice is shown in (a) Dodo-Goldilocks and (b) Upper Cupboard trenches and icy soil is shown in (c) Neverland, (d) Snow White, and (e) La Mancha trenches. Chatter marks (horizontal groves and ridges observed on all icy exposures), light and dark toned material that changes brightness or recedes over time, and RA motion impedance helped to determine the occurrence of ice. In the Snow White trench (Figure 2d), scraping the ice table with the secondary blade exposed a large area of dark toned ice-cemented soil. In addition, the soils in La Mancha (Figure 2e) appeared weakly cemented and cloddy above the ice table. Images are SS019IOF897905015_127-FERCBA1TB (trench ~21 cm wide) (Figure 2a), SS114IOF906342294_1D450R2CBA18TB (trench ~15 cm wide) (Figure 2b), SS071IOF902531496_18110R2CBA18TB (trench ~8 cm wide) (Figure 2c), SS045IOF900218735_15030R2CBA18TB (trench ~23 cm wide) (Figure 2d), and SS148IOF909363226_20560RCBA1TB (scene width ~52 cm) (Figure 2e).

to roughen with time and close-up views of Snow Queen showed centimeter-scale fracturing, erosion and degradation [*Keller et al.*, 2009; *Markiewicz et al.*, 2009] (see also Figures 3c and 3d). In addition, the entire surface of Holy Cow, which was subjected to high midday insolation, was observed to undergo deflation between sols 8 (L_S 80°) and 142 (L_S 143°), evidenced by a downward shift in the contact between the icy surface and the pit walls along the entire southern perimeter (see Figures 3e and 3f). The magnitude of this deflation is estimated to be about 6 mm ± 3 mm. Though significant roughening and degradation of the surface of Snow Queen was observed, which received limited insolation during nighttime hours, no general deflation could be easily discerned.

[14] To examine the stability of ground ice, a collection of 91 study points were identified across all the trenches. The

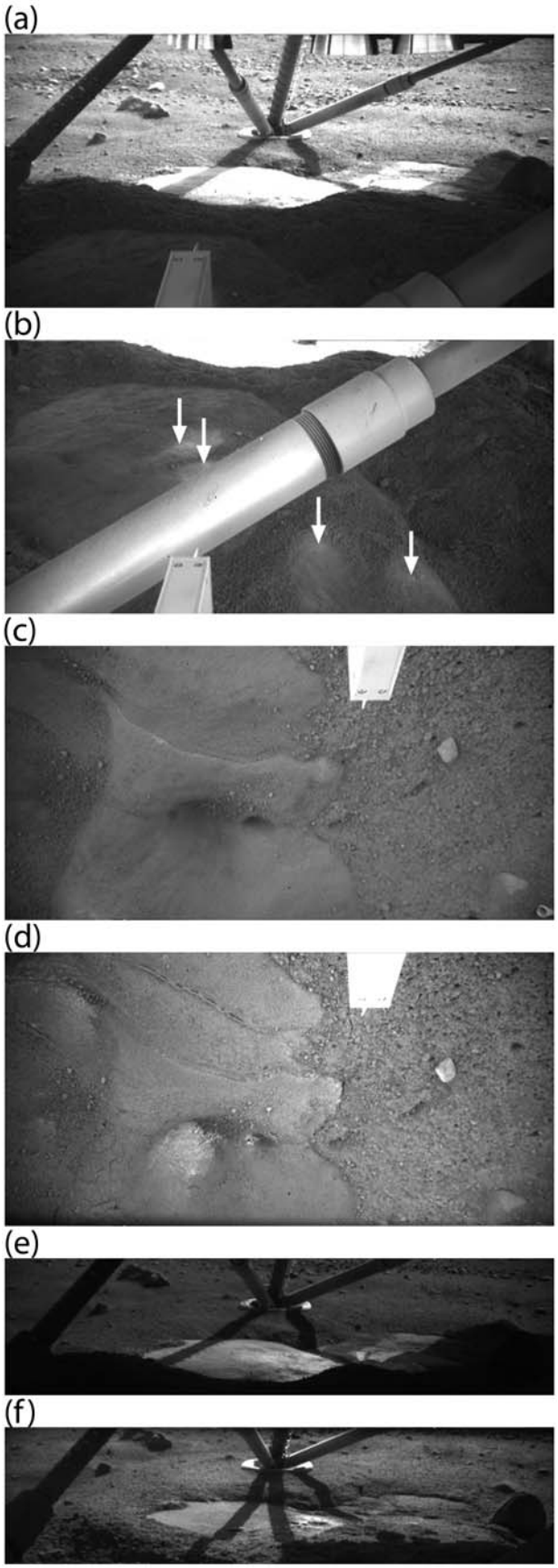

distribution of study points is inherently nonrandom as trench locations were chosen to examine specific characteristics of the landing site and polygonal terrain, and points within the trenches were selected to examine specific exposed areas of interest (e.g., ice-rich material). Additional points were discarded, due to the proximity of surface rocks complicating topographic analysis. For each study point the depth of the ice table and predig surface slope was determined from stereo imaging. Figure 4 shows the distribution of points. Each SSI stereo pair was processed to produce a range map [*Alexander et al.*, 2006], and range maps were mosaicked into a digital elevation model (DEM). The elevation of the initial surface and the elevation of the floor of the trench when ice was first encountered (or total depth excavated) were differenced for each study point to determine the vertical depth of the ice table. Pretrenching and posttrenching elevations were taken as the median over a 1 cm^2 area centered on the study point. The initial north-south surface slope prior to trenching was also determined from the median slope over a 10 cm (north-south) baseline across a 2 cm (east-west) area, as this is an important factor in the mean surface and subsurface temperatures which control ice stability. A 10 cm baseline was chosen to average out surface roughness and to minimize the effect of surface curvature. East-west slopes and shadowing from microtopography may also affect the mean soil temperatures, but to a lesser degree and are not considered here.

[15] Depths and slopes for each study point are given in Tables 1–3 for light toned ice, icy soil, and points not deep enough to reach confirmed ice, respectively. Uncertainties in measured depths are estimated at ±3 mm and in slopes at ±1°. Histograms of ice table depths are shown in Figure 5. The shallowest point to icy soil was in Snow White at 1.3 cm on largely level ground in the center of a polygon mound. The deepest point believed to be the ice table was 11.2 cm in the lower portions of Dodo-Goldilocks on a south facing shoulder of a polygon trough. The deepest point excavated was in Stone Soup at 18.3 cm without definitively reaching icy material. The mean depth measured of all icy soil points was 4.6 cm, and 3.7 cm for the light toned ice alone. For comparison, the distance of the floor of the Holy Cow thruster pit to the ledge of soil next the foot pad (Figure 3a) is about 5.5 ± 0.6 cm, however soil deposition around the footpad during landing would make

Figure 3. Views of ground ice exposed in ~50 cm pits by the descent thrusters under the lander. (a, e, and f) The feature Holy Cow near the southern footpad. Changes in the surface of Holy Cow sol 8 (Figure 3e) and sol 142 (Figure 3f) suggest deflation of the surface by about 6 mm. (b–d) Different views of the feature Snow Queen and ice cemented soil textures. Arrows in Figure 3b show where the thrusters impinged the surface. Changes in the surface of Snow Queen between sol 21 (Figure 3c) and sol 142 (Figure 3d) show fracturing and degradation, presumably by sublimation of ice cement, but do not indicate any significant deflation. Images are RS005EFF896663219 (Figure 3a), RS008EFF896930575 (Figure 3b), RS021EFF898085446 (Figure 3c), RS142EFF908818863 (Figure 3d), RS008EFF896930467 (Figure 3e), and RS142EFF908818700 (Figure 3f).

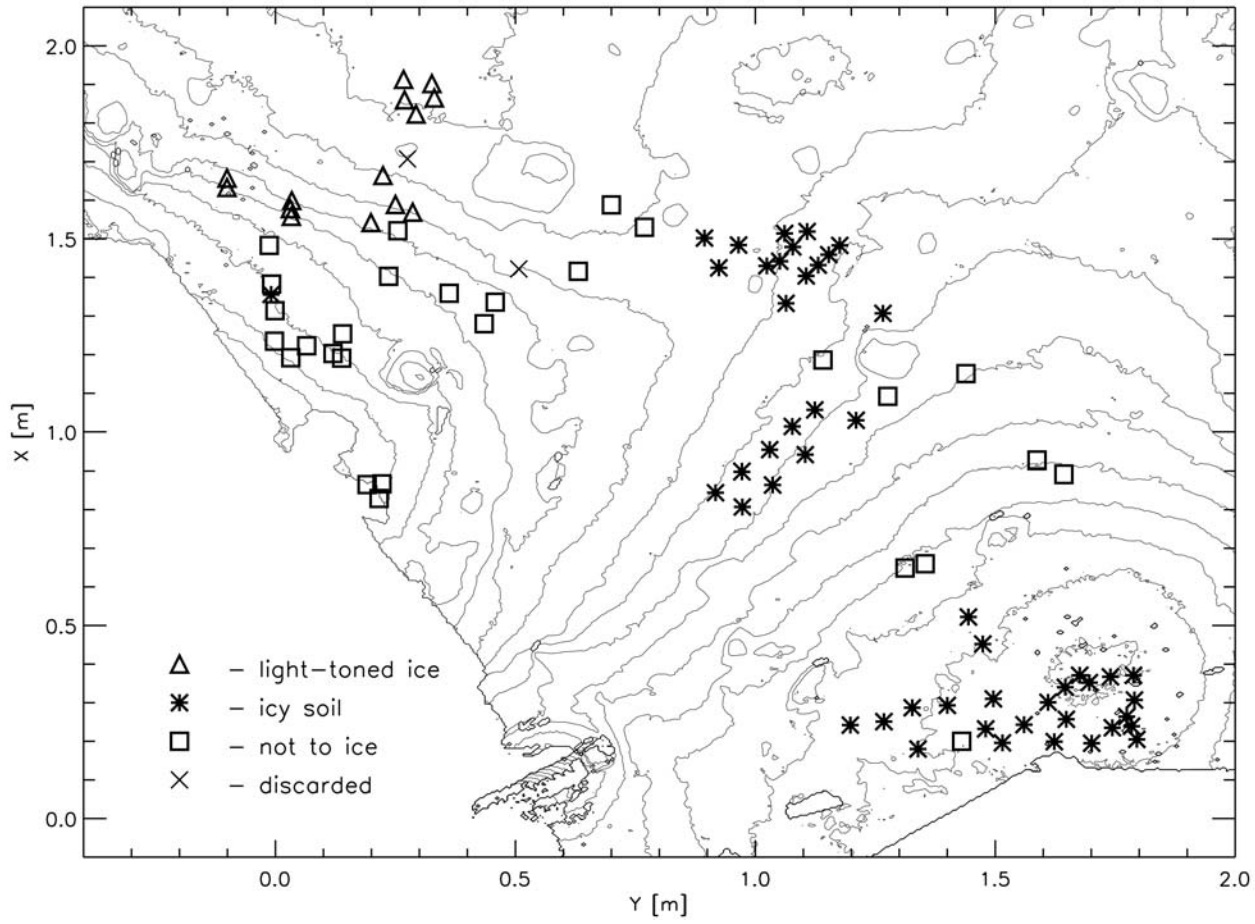

Figure 4. Map showing the spatial distribution of study points around the work space. Light toned ice (triangle) was exposed in the northwest corner of the work space, while icy soil (asterisk) occurred elsewhere. Points where ice was not encountered either did not exhibit clear evidence of ice or digging was limited by mission operations. Two discarded points are noted (cross) where light toned ice was encountered, but depth and slope data were not available, each due to the ice being located under a multicentimeter rock. Contours represent a preexcavation topographic map of the work space at 2 cm intervals.

Table 1. Light Toned Ice Study Points[a]

Trench	X (North) (m)	Y (East) (m)	Ice Table Depth (cm)	South Slope (deg)	Best Thermal Inertia (J m^{-2} K^{-1} $s^{-1/2}$)	Best Vapor Density (10^{19} m^{-3})
DG	1.657	−0.101	2.9	20.6	82	26.4
DG	1.633	−0.101	2.8	19.3	91	24.8
DG	1.578	0.031	4.5	17.7	118	16.2
DG	1.599	0.034	4.2	17.5	118	16.6
DG	1.558	0.033	3.7	18.5	105	19.3
UC	1.823	0.293	3.1	1.6	211	5.9
UC	1.913	0.267	3.2	−0.1	223	5.0
UC	1.902	0.326	3.6	−0.8	238	4.0
UC	1.860	0.269	3.4	2.3	216	5.5
UC	1.865	0.331	3.4	0.7	224	4.8
UC	1.664	0.224	4.2	10.8	170	9.5
UC	1.589	0.250	4.1	14.2	141	12.9
UC	1.542	0.199	4.7	16.2	133	14.0
UC	1.569	0.286	4.4	14.8	140	13.0

[a]Trench names are BA, Burn Alive; BL, Bears Lodge; DG, Dodo-Golidlocks; IM, Ice Man; LM, La Mancha; LC, Lower Cupboard; N, Neverland; PD, Pet Donkey; RA, Run Away; SS, Stone Soup; SW, Snow White; UC, Upper Cupboard. Ice table depth uncertainties are ±3mm. Slope uncertainties are ±1°. Best thermal inertia assumes a vapor density of 3.4×10^{19} m^{-3}. Best vapor density assumes a thermal inertia of 250 J m^{-2} K^{-1} $s^{-1/2}$.

Table 2. Ice-Cemented Soil Study Points[a]

Trench	X (North) (m)	Y (East) (m)	Ice Table Depth (cm)	South Slope (deg)	Best Thermal Inertia (J m^{-2} K^{-1} $s^{-1/2}$)	Best Vapor Density (10^{19} m^{-3})
DG	1.356	−0.009	11.2	5.6	315	1.4
LM	1.502	0.894	6.7	1.9	289	2.0
LM	1.484	0.965	6.5	3.0	275	2.4
LM	1.425	0.924	6.5	0.9	294	1.8
LM	1.479	1.078	6.8	−0.2	309	1.5
LM	1.430	1.024	6.5	0.1	301	1.7
LM	1.442	1.051	6.8	0.8	300	1.7
LM	1.432	1.131	5.6	0.8	277	2.3
LM	1.333	1.064	6.3	−0.4	300	1.7
LM	1.519	1.108	6.3	−4.5	325	1.1
LM	1.514	1.061	5.9	−0.7	294	1.8
LM	1.483	1.176	5.8	−3.7	309	1.5
LM	1.459	1.153	5.4	−1.4	287	2.0
LM	1.404	1.106	5.5	0.4	278	2.3
N	1.057	1.124	4.3	−7.5	285	2.1
N	1.014	1.077	3.5	−4.4	249	3.5
N	0.954	1.030	4.3	−5.6	278	2.3
N	0.898	0.972	5.4	−5.2	307	1.5
N	0.844	0.917	5.2	−7.8	312	1.4
N	1.030	1.210	4.2	−8.0	283	2.1
N	0.941	1.104	4.4	−7.3	287	2.0
N	0.864	1.036	5.6	−3.7	304	1.6
N	0.807	0.973	5.7	−6.1	319	1.3
PD	1.307	1.266	5.1	−3.8	293	1.9
BA	0.522	1.444	3.0	−6.7	238	4.0
BA	0.452	1.474	3.0	−3.5	229	4.6
SW	0.371	1.788	4.3	1.8	241	3.9
SW	0.367	1.740	5.1	1.8	259	3.0
SW	0.352	1.696	4.1	2.9	229	4.5
SW	0.340	1.646	4.1	3.4	225	4.8
SW	0.307	1.790	4.3	−5.6	278	2.3
SW	0.264	1.774	4.3	3.2	231	4.4
SW	0.257	1.648	3.3	10.5	158	11.3
SW	0.243	1.560	2.8	2.8	195	7.3
SW	0.371	1.676	5.1	3.1	248	3.5
SW	0.239	1.784	4.7	9.5	188	7.7
SW	0.205	1.795	4.0	2.2	231	4.4
SW	0.235	1.744	3.6	10.7	162	10.7
SW	0.195	1.701	2.4	0.8	192	7.7
SW	0.199	1.623	3.4	−5.9	250	3.4
SW	0.301	1.610	3.4	4.1	205	6.4
SW	0.293	1.400	3.2	−2.3	231	4.5
SW	0.287	1.327	2.6	0.7	199	6.9
SW	0.180	1.339	2.5	0.9	195	7.3
SW	0.310	1.496	2.6	1.2	197	7.2
SW	0.196	1.515	3.3	3.1	208	6.1
SW	0.232	1.480	2.6	1.9	194	7.5
SW	0.251	1.268	1.3	−0.3	147	13.7
SW	0.242	1.198	2.4	0.3	194	7.4

[a]See Table 1 footnotes.

this an over estimate and in better agreement with the trenched depths. Slopes at the study points ranged from 12° poleward to 20° equatorward. The light toned ice in Dodo-Goldilocks and in Upper Cupboard was observed to have a relatively abrupt southern perimeter, where trenched depths increased rapidly over a distance of a couple of centimeters.

3. Analysis of Ice Stability

[16] The current stability or instability state of ground ice at the Phoenix site provides a window into its history and the physical processes which control it. Ground ice could be emplaced by a variety of mechanisms and evolve over time. Stability, specifically with respect to sublimation and diffusive exchange with the atmosphere, has been considered for decades to be the primary process controlling its distribution on a regional scale. However, on the scale of the Phoenix work space the depth of an ice table in diffusive equilibrium can vary due to a variety of factors. Key factors controlling the stability and depth of ground ice are thermal inertia, albedo, and surface slope which collectively control subsurface temperatures, as well as the average absolute humidity of the near surface atmosphere (expressed as a molecular density, m^{-3}) which controls molecular diffusion and diffusive equilibrium [see also *Mellon et al.*, 2004]. Annual average vapor densities are typically considered because diffusion time scales for the loss or gain of ground ice are much longer than a year [e.g., *Mellon and Jakosky*, 1993]. Using observed properties, the measured ice table depths and its variability can be compared with the theo-

Table 3. Study Points Not Excavated to Ice[a]

Trench	X (North) (m)	Y (East) (m)	Depth (cm)	South Slope (deg)
DG	1.483	−0.013	10.2	12.2
DG	1.383	−0.008	12.6	5.6
DG	1.314	−0.001	12.6	5.0
SS	1.254	0.140	16.1	6.0
SS	1.203	0.120	17.5	7.0
SS	1.191	0.138	18.3	7.3
SS	1.223	0.065	15.9	8.0
SS	1.235	−0.002	15.9	10.9
SS	1.192	0.032	15.7	11.7
UC	1.521	0.255	7.0	15.5
UC	1.403	0.236	8.7	9.7
LC	0.865	0.191	6.5	−2.2
LC	0.829	0.216	7.3	−7.1
LC	0.867	0.222	7.4	−1.7
IM	1.336	0.458	8.1	8.2
IM	1.280	0.435	9.6	2.8
IM	1.359	0.362	8.2	8.7
LM	1.588	0.700	4.4	1.8
LM	1.416	0.631	7.6	6.3
LM	1.530	0.769	5.9	3.6
PD	1.186	1.141	5.2	−4.4
PD	1.092	1.276	3.8	−2.1
PD	1.151	1.439	6.8	−5.2
BL	0.660	1.354	2.0	−4.9
BL	0.649	1.312	3.9	−6.6
RA	0.927	1.587	1.4	−10.4
RA	0.891	1.643	2.5	−12.2
SW	0.200	1.430	2.9	2.8

[a]See Table 1 footnotes.

retical depths. The objective of this section is to examine the stability state of the ice, to understand the average conditions under which the observed ice distribution would be stable and its variability over the work space. Rocks can create large thermal perturbations affecting the ice table and are examined by *Sizemore et al.* [2009].

[17] A difficulty with interpreting the ice table depth observations is that the landing thrusters caused a redistribution of soil around the lander. Within the work space evidence of both deposition and scouring are observed, making interpretations of ice table depth somewhat confused. Roughly 5×10^4 cm^3 of soil was excavated from the thruster pits under the lander. Models show that as much as a few cm of soil would be deposited close to the lander, decreasing exponentially outward across the work space [*Mehta et al.*, 2008]. Evidence of this deposition can be seen in the form of rough soil textures, rocks embayed with soil on their lander side, and rocks topped with soil. The trenches Stone Soup and Lower Cupboard are most likely affected by this deposition, which are also the deepest trenches explored without finding ice, as well as the southwest end of Neverland where the ice table is observed to deepen closer to the lander.

[18] Erosion and scouring is also evident in the area of Dodo-Goldilocks and the southern portion of Upper Cupboard representing the shoulder of a polygon trough. Figure 6 shows the soil in these areas marked by fluting and pits, rocks appearing undercut (as apposed to embayed by soil), and displacement of decimeter-scale rocks by more than 1/2 m. This area is of particular interest as an exposure of shallow light toned ice occurs here. The southern edge of this light toned deposit appears to correlate with the boundary between apparent erosional and depositional morphologies (see Figures 6 and 2a). Pretrench stereo images at this location indicate south facing slopes up to 20°. However, if erosion of as little as 1−2 cm of soil occurred preferentially from the lower portion of the slope, the slope that existed prior to landing may have been closer to 10°. The median slope in the polygonal terrain around the lander is about 7° [*Mellon et al.*, 2009] and slopes approaching 20° are rare. Therefore, in examining the depth of the ice table in relation to the Martian climate, we will focus on points further from the spacecraft where erosion and deposition effects are believed to be minimal. Figures 7a and 7b show histograms of measured values of ice table depth and surface slope for all the study points where ice was exposed. The occurrence of high slopes, over 10°, is noted by gray bars.

[19] In addition to slope, thermophysical properties of the ice-free surface layer are important to understanding the stability of ground ice in the present and past climates. The albedo is estimated to be about 0.20 with little observed variation over the work space, the landing site, or the

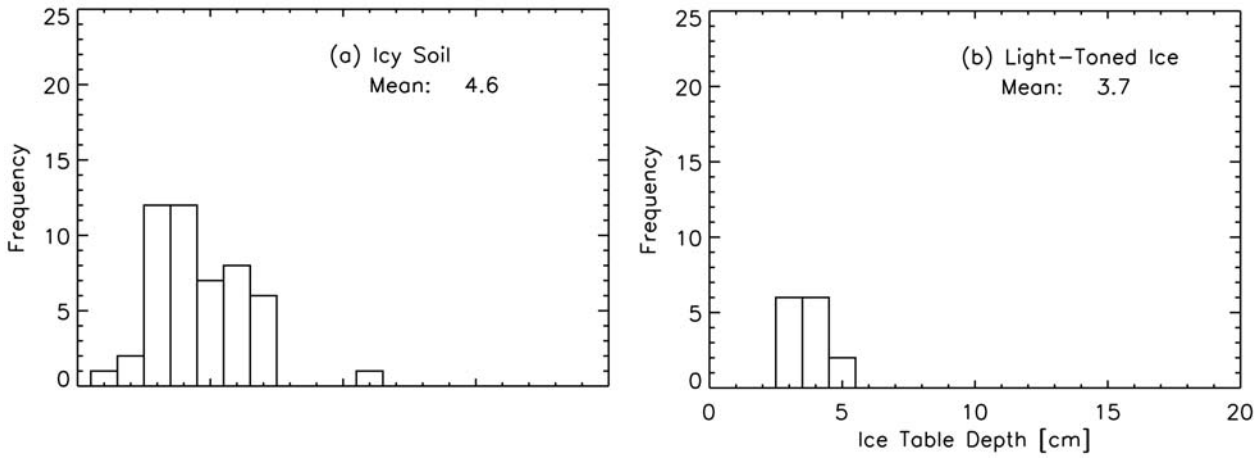

Figure 5. Histograms of depth of the ice table for the collection of study points: (a) ice-cemented soil and (b) light toned ice. Depths are listed in Tables 1 and 2.

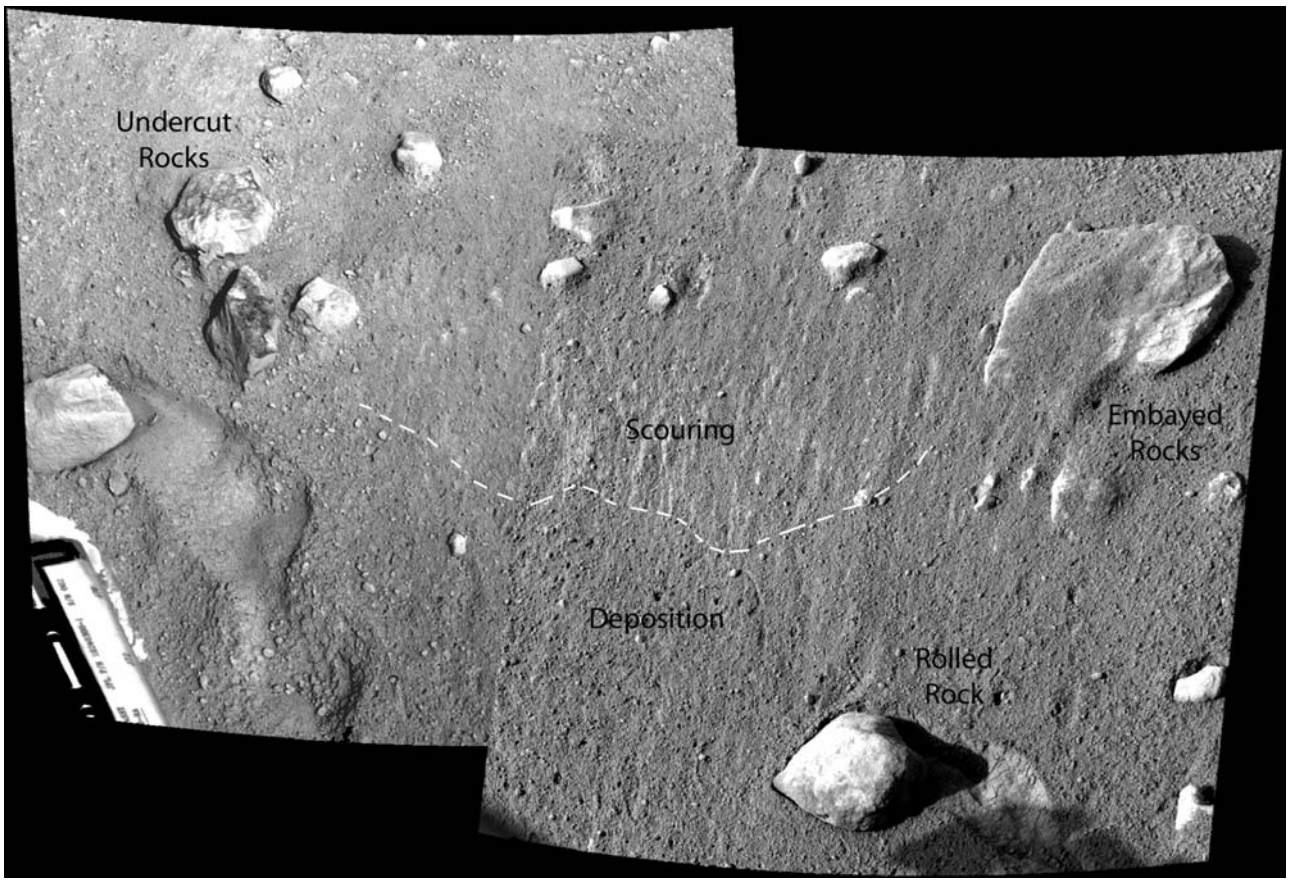

Figure 6. Scouring in the Dodo-Goldilocks and lower Upper Cupboard region prior to excavating trenches. The boundary (dashed line) indicates a transition in surface texture, between fluted, pitted above, and particulate, rough below. Light toned ice in the Dodo-Goldilocks and lower Upper Cupboard trenches occurs in the fluted area, for which ice table depths and surface slopes would have been altered during landing. Outside this scouring zone the ice table deepens. Two decimeter-scale rocks were slid or rolled by the thrusters illustrating the strength of erosive forces in this area.

region. Thermal inertia was derived from low-resolution orbit-based brightness-temperature observations and in situ for the first time by Phoenix's Thermal and Electrical Conductivity Probe (TECP) attached to the end of the RA (see *Zent et al.* [2009] for complete analysis of TECP results). Orbit-based derivations are complicated by the presence of shallow ground ice, but are typically fit by a low thermal inertia particulate layer (about 183–223 J m^{-2} K^{-1} $s^{-1/2}$ [*Titus and Prettyman*, 2007; *Putzig and Mellon*, 2007]) over high thermal inertia ground ice. TECP measurements of the ice-free soil overburden provide average thermal properties over the top 15 mm of the soil. Results indicate a range from about 200 to 350 J m^{-2} K^{-1} $s^{-1/2}$, varying mainly with diurnal soil temperature, but with some variability between measurement sites around the work space. In general, higher thermal inertia surfaces will have higher annual mean temperatures and result in deeper ice table equilibrium depths relative to low thermal inertia surfaces [e.g., *Paige*, 1992]. Likewise equatorward sloped surfaces will be warmer and the ice table will be deeper than for poleward slopes [e.g., *Aharonson and Schorghofer*, 2006].

[20] Figure 8 shows the ice table depth (and the depth excavated where no ice was encountered) for all study points as a function of the initial surface slope. Superimposed are the theoretical equilibrium ice table depths assuming the annual average atmospheric water vapor density of 3.4×10^{19} m^{-3} (see below) based on the methods of *Mellon et al.* [2004, and references therein]. Most of the study points agree well with the theory, following the same trend with slope and for a reasonable range of thermal inertias. There are two outliers to consider further. First, a collection of light toned ice points are shown with a high equatorward slope and therefore an unusually shallow depth relative to equilibrium models. These points are located in Dodo-Goldilocks and the lower parts of Upper Cupboard in the area of scouring discussed above, and if the altered slope and erosion of soil are taken into account, these points would shift to greater depths and lower slopes to follow the same trend as the other icy points. Second, the deepest points for each range of slope are also in areas of the largest soil deposition from the thrusters in Lower Cupboard, Stone Soup, and Ice Man. While all but one of these points did not expose ground ice, the trench depths are likely deeper by a few cm than would represent the prelanding soil surface.

[21] The results in Figure 8 show that the relationship between our two measured quantities (ice table depth and

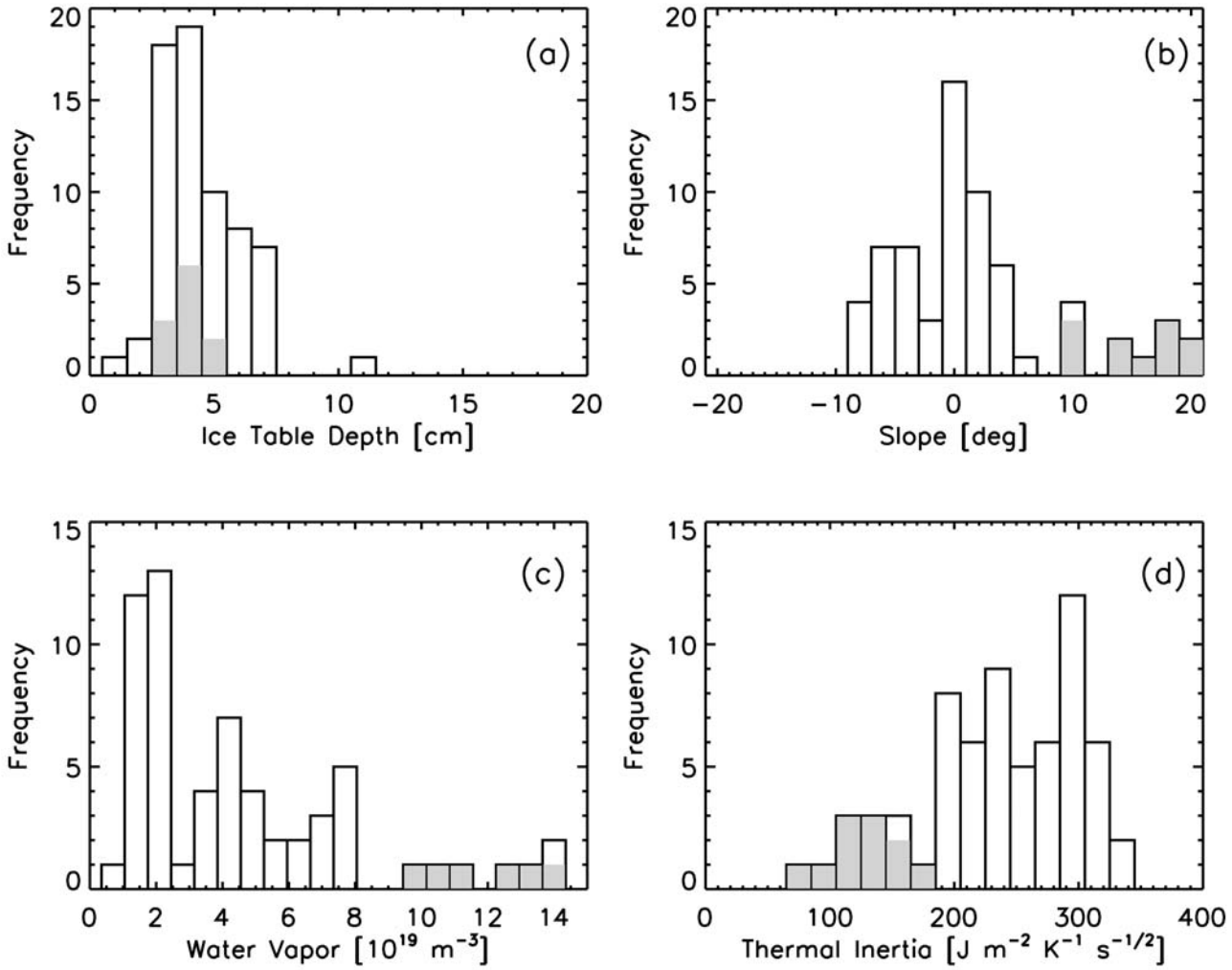

Figure 7. Histograms of all study points of icy material noted in Tables 1 and 2 showing (a) ice table depth, (b) surface slope, (c) best fitting water vapor density assuming a thermal inertia of 250 J m^{-2} K^{-1} $s^{-1/2}$, and (d) best fitting thermal inertia assuming a water vapor density of 3.4×10^{19} m^{-3}. Gray indicates the fraction of points with slopes greater than 10° in the scoured region noted in Figure 6.

surface slope) behaves approximately according to theoretical models of atmosphere/ground ice equilibrium [*Mellon et al.*, 2004]. However, to investigate the stability of the ice further we consider that for each study point we have two remaining unknowns, the average atmospheric water vapor density and the thermal inertia of the ice-free soil overburden. First, while all points should be exposed to approximately the same atmospheric water vapor boundary condition, we do not know exactly what that value should be. Current day measurements may not be appropriate, as water vapor diffusion through the soil overburden is slow and ground ice equilibrium generally represents 100 to 1000 year time scales. Second, while we have direct measurements of the thermal inertia of the ice-free overburden, we do not have measurements for each study point individually and not a complete integration of thermal inertia at all depths from the surface to the ice table. Some spatial (and vertical) variability is expected due to small variations in soil cementing, particle size sorting, bulk density, etc. Analysis of RA forces indicate that stratigraphy in the soil cohesion is present and varies from trench to trench [*Arvidson et al.*, 2009; *Shaw et al.*, 2009]

[22] If we assume the thermal inertia is approximately a midrange value as observed by the TECP (we choose 250 J m^{-2} K^{-1} $s^{-1/2}$ consistent with seasonal temperatures), we can estimate the average atmospheric water vapor density needed to achieve diffusive equilibrium for each study point using an equilibrium ice stability model [*Mellon et al.*, 2004]. Figure 7c shows a histogram of the resulting atmospheric vapor densities for the measured values of ice table depth and surface slope, and the assumed thermal inertia (see also Tables 1 and 2). Water vapor densities are scattered over more than an order of magnitude, from about 1×10^{19} to 1.3×10^{20} m^{-3} for icy study points, avoiding the scoured area (Figure 6). Since the surface would be exposed to essentially the same atmosphere everywhere, these variations cannot be explained by local variations in average water vapor and must result from deviations in thermal inertia from the

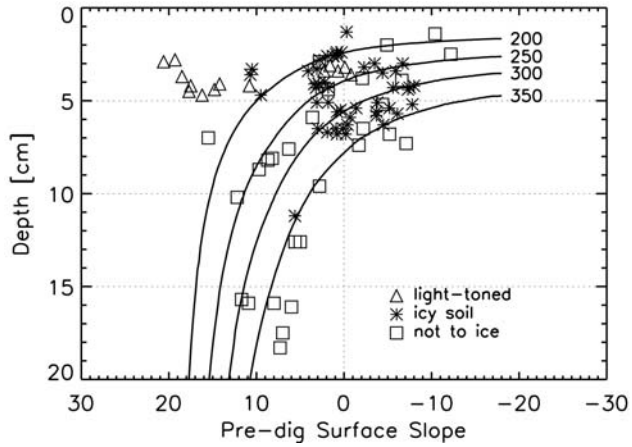

Figure 8. Ice table depths as a function of surface slope for the trench study points. Lines represent the theoretical trend for different thermal inertias of the overburden soil [*Mellon et al.*, 2004] in J m^{-2} K^{-1} $s^{-1/2}$. Most points fall within the observed range of thermal inertia. The high-slope surfaces underlain by light toned ice fall outside the range of models toward lower thermal inertias, but these surfaces show evidence of significant scouring (Figure 6).

assumed value of 250 J m^{-2} K^{-1} $s^{-1/2}$. The mean water density for these study points is 3.4×10^{19} m^{-3}.

[23] This vapor density represents an annual mean boundary condition that subsurface ice experiences in order to be in diffusive equilibrium with the atmosphere, and interpretation of this value is complicated by the seasonal temperature cycles and the potential for surface saturation relative to the atmosphere. These saturation effects have been modeled in various ways, the most direct of which has been to numerically simulate the surface temperatures as compared to the atmospheric frost point and allow surface saturation to dry the near-surface atmosphere [e.g., *Mellon and Jakosky*, 1993; *Chamberlain and Boynton*, 2007]. Integrating this saturation effect for the Phoenix landing site indicates that a summertime average near-surface vapor density of 11.8×10^{19} m^{-3} is required to achieve an annual average of 3.4×10^{19} m^{-3}. Converting the summertime average to a more familiar column abundance by assuming water is well mixed with CO_2 at the Phoenix elevation, 11.8×10^{19} m^{-3} translates to about 38 pr μm (precipitable microns) in excellent agreement with TECP humidity measurements for the current climate [*Zent et al.*, 2009]. This result indicates that the current atmospheric water vapor abundance in the northern plains is representative of the conditions for the past 100–1000 year time scales.

[24] If we now assume the water vapor abundance experienced by all points is 3.4×10^{19} m^{-3}, we can derive the thermal inertia needed to achieve diffusive equilibrium. Results are shown as a histogram in Figure 7d and in a map view in Figure 9. Excluding the scoured region (Figure 6), the resulting thermal inertias range from about 190 to 325 J m^{-2} K^{-1} $s^{-1/2}$ (see also Tables 1 and 2). The mean values is 250 J m^{-2} K^{-1} $s^{-1/2}$, which of course is entirely circular. However, the range represented here can result from particle size variations between several tens and a few hundred microns [e.g., *Presley and Christensen*, 1997] or variations in mineral cementation of zero to less than 1% [see *Mellon et al.*, 2008c], with grains sizes consistent Optical Microscope (OM) results [*Pike et al.*, 2008]. From the map view in Figure 9, the higher thermal inertias occur in the shallow trough (La Mancha), a location where particularly cloddy soils were observed at depth (see also Figure 2e). Lower thermal inertias are indicated in the polygon mounds (Snow White and Upper Cupboard).

[25] Other factors may also play a role in the stability of ice. Soluble salts can reduce the water vapor pressure in equilibrium with the ice at the ice table and allow ice to persist at lower atmospheric water abundances at a given depth. Small amounts of carbonate [*Boynton et al.*, 2009] and perchlorate salts [*Hecht et al.*, 2009] have been detected, uniformly distributed within the soil overburden at concentrations of approximately 1%. No concentrated or heterogeneous distributions of salts are implied by these observations, nor indicated in spectral data [*Blaney et al.*, 2009]. This amount of salt is not likely to play a role in defining the depth of the ice table, unless it were to become concentrated. Lateral heat conduction may also play a role where the thermal properties of the soil vary laterally on decimeter scales, causing local cooling or warming and deviation in the ice table depth relative to the depth that would be dictated by the properties of the immediately overlying soils; however, for the range of soil thermal inertia values observed, this deviation will not amount to more than a few millimeters. This effect can be particularly important in the neighborhood of a rock [*Sizemore and Mellon*, 2006; *Sizemore et al.*, 2009].

[26] Throughout this discussion, we have assumed that ice is generally in equilibrium with atmospheric vapor and looked for consistency with this assumption and areas of deviation that would imply disequilibrium. Results are largely consistent with the ice table being in diffusive equilibrium with atmospheric water vapor, and consistent with a large body of previous studies (see *Mellon et al.* [2008a] for a review) and with the examination of the ice table profile under rocks at the landing site [*Sizemore et al.*, 2009]. The light toned ice in the areas of Dodo-Goldilocks and the lower portion of Upper Cupboard at the depths and slopes measured, would require extremely low thermal inertias (in some instances below 100 J m^{-2} K^{-1} $s^{-1/2}$) to be in equilibrium. Such low thermal inertias can only occur in unconsolidated fines with mean particle sizes of a few microns, inconsistent with OM results indicating typically $\sim$70–80 μm particles which are consistent with our adopted mean TECP thermal inertia of 250 J m^{-2} K^{-1} $s^{-1/2}$ [*Pike et al.*, 2008]. Using this higher thermal inertia the light toned ice in this location would be out of equilibrium and would sublimate at a rate of about 3.5 mm/yr (assume water vapor diffusing through soil [see *Mellon and Jakosky*, 1993; *Sizemore and Mellon*, 2006]). As discussed above, the removal of 1–2 cm of soil from this location by the decent thrusters is entirely consistent with the ice in this region being forced out of equilibrium during landing.

4. Origins of Shallow Ground Ice

[27] Ground ice at the Phoenix landing site occurs in two distinct forms implying their origins are equally varied. The ice table over most of the work space and much of what we can discern under the lander is composed of a

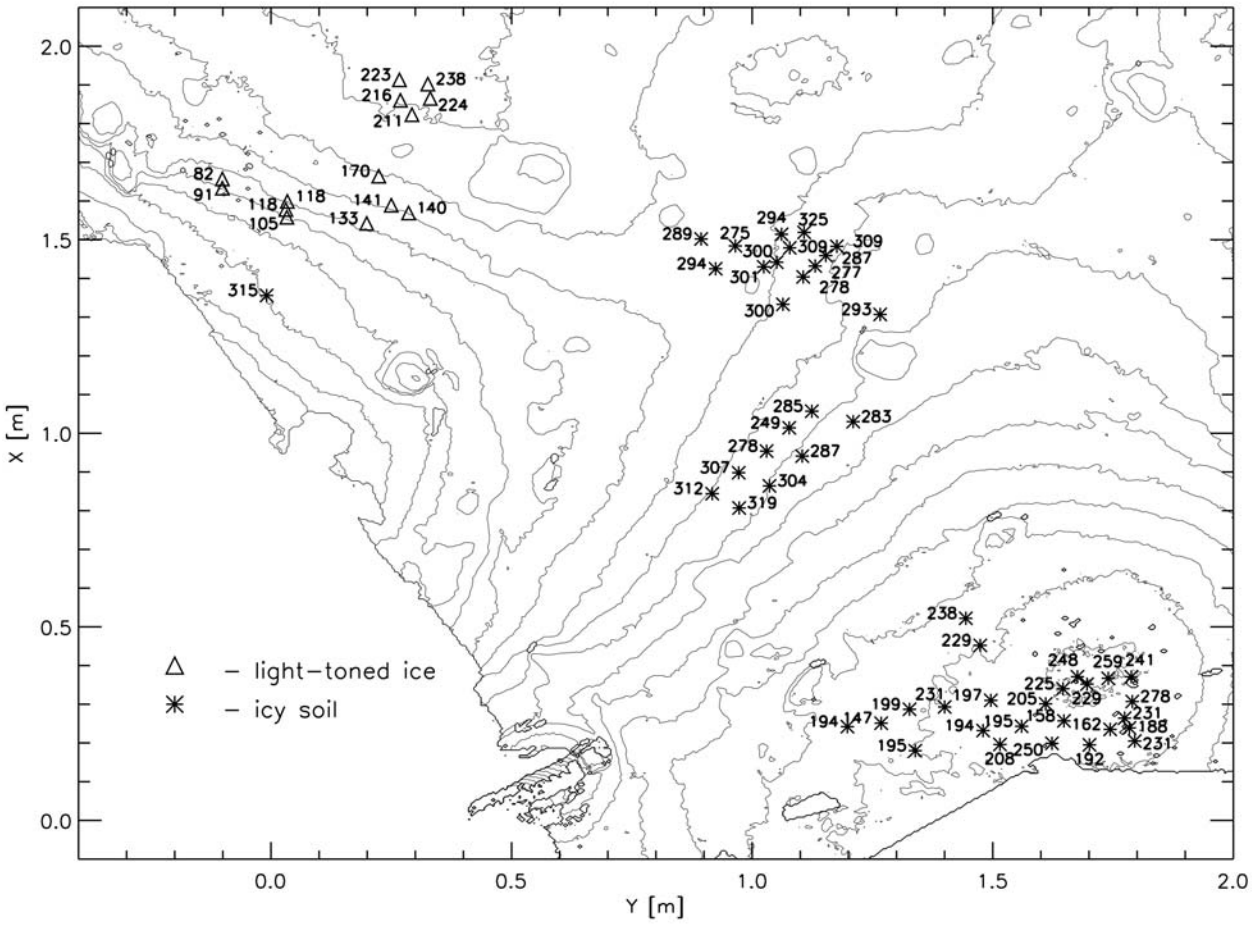

Figure 9. Map of the best fitting thermal inertia of the overburden soil assuming a water vapor density of 3.4×10^{19} m^{-3}. Thermal inertia values are given in units of J m^{-2} K^{-1} s$^{-1/2}$. Lower values occur in the soils of the polygon interiors, while higher values occur in the polygon trough regions. The lowest values occur in the scoured region (Figure 6).

matrix-supported ice-saturated soil. Over a small region of the work space occurs a light toned ice that appears to be porous, nearly pure ice. In this section we will consider possible origins for these ice deposits and place Phoenix ground ice observations into context with the rest of Mars.

[28] It is believed that over orbital cycles (obliquity, eccentricity, perihelion) and associated climate cycles that the equilibrium ice table depth will undergo oscillations over geologic history [*Mellon and Jakosky*, 1995; *Chamberlain and Boynton*, 2007; *Zent*, 2008]. During these climate cycles and at high latitude the ice table can cyclically recede by desiccation to depths of several decimeters or more. The present-day depth of the ice table is relatively shallow, ~4–5 cm. Therefore, ice present at the ice table and below to the depth of cyclic desiccation should be geologically young, perhaps only 100 kyr, forming under recent climate condition.

[29] Ice-saturated soil appears to be the dominant form of ice, representing about 90% of the ground ice exposed by trenching operations. It occurs in the interior mound and flanks of the Wonderland polygon, across to the shallow trough in the trench La Mancha, and in a larger trough at the south end of Dodo-Goldilocks. Close examination of the ice table in the Snow White trench revealed a hard and generally dark toned icy material when scraped clean of loose soil, indicating pore saturation. Sublimation of the ice over several sols resulted in a millimeter-scale soil lag that could be scraped off, otherwise exhibiting no visible signs of deflation, suggesting the soil matrix can support its own weight [*Morris et al.*, 2008]. OM analysis of the lag and ice-free soil overburden [*Pike et al.*, 2008] suggests no significant difference in soil particles above and below the ice table. The volumetric heat capacity of the overburden soil was measured by the TECP to be about 1×10^6 J m^{-3} K^{-1}, and assuming basaltic mineralogy implies a soil porosity of 50–55% [*Zent et al.*, 2009]. Examination of the icy exposure in Snow Queen showed fractures beginning to form in the sublimation lag after 41 sols [*Markiewicz et al.*, 2009], suggesting a small amount of grain-to-grain contraction accompanying the water loss.

[30] These observations indicating pore ice are entirely consistent with vapor diffusion and condensation of ice in the pores of the existing soil. This style of ice emplacement process does not require climate conditions different than those observed today. Alternatively, pore ice can form during freezing of liquid water in a soil. If the initial soil were saturated with water, the 9% expansion of water during freezing would exceed the pore volume. Excess ice

structures millimeters to centimeters in scale, such as ice lenses, could also form [e.g., *Taber*, 1929]. If such structures existed at the ice table, sublimation after trenching would have resulted in some subsidence. Ultimately, excavation deep below the ice table may be necessary to determine if such structures are truly present or not. Nonetheless, observations do not suggest excess ice is present and support the vapor deposition of pore ice. This pore ice, and not massive clean or dirty ice, is believed to dominate the subsurface to depths of at least 10–15 m, based on analysis of polygon size and fracture formation theory [*Mellon et al.*, 2008b, 2009]. Polygon trough morphology is also inconsistent with significant sublimation degradation of the landscape, as would occur if shallowly buried clean ice became periodically unstable [*Mellon et al.*, 2009].

[31] Light toned ice occurs in only a fraction of the excavated areas, primarily on the south flank of the Humpty Dumpty polygon. While not the dominant form of ice, it is unusual and raises interesting questions about the formation and history of the ice. In general, this ice can be characterized as weaker or more friable than the ice-saturated soils. It has a low soil content, 1–2%, containing similar particles to the overburden soil, but with more sand sized grains. It is lighter toned than other ices or loose soils, implying visible light scattering by air pockets and gaps between small ice crystals. However, darker and more translucent regions within this ice also occur, indicating areas of more dense ice [*Smith et al.*, 2009; *Blaney et al.*, 2009; *Morris et al.*, 2008]. Unlike the formation of pore ice, such excess ice deposits in the subsurface cannot be easily attributed to condensation of ice directly from water vapor in the Martian subsurface, and other processes need to be considered. Additionally, the size and morphology of polygonal ground indicates that ice-cemented soils dominate the subsurface [*Mellon et al.*, 2008b, 2009], and that pure ice deposits must be localized phenomena precluding their origin as a massive buried remnant of an ancient glacial deposit or frozen sea.

[32] There are a number of endogenic processes that can form excess ice in the subsurface and in situ segregation of ice and soil. Perhaps the most common form of excess ice in terrestrial permafrost are ice lenses, thin veins of clean ice that form parallel to the surface as wet soil freezes [e.g., *Taber*, 1929; *Williams and Smith*, 1989]. Needle ice, common in terrestrial temperate regions during an overnight freeze, occurs close to the soil surface as growing individual ice crystals push soil grains apart [e.g., *Soons and Greenland*, 1970; *Washburn*, 1980]. In both cases, the availability of liquid water is important for rapid ice formation; however, thin interfacial films play a crucial role in water transport into the zone of crystal growth [*Miller*, 1980, *Miller and Black*, 2003]. In the current climate (or recent climates) at the Phoenix landing site, surface and subsurface temperatures are not expected to support the presence of liquid water [*Mellon et al.*, 2008a], but do support the formation of thin films of adsorbed water [e.g., *Zent*, 2008; *Zent et al.*, 2009]. These films are known to be mobile at temperatures well below freezing [*Anderson and Tice*, 1972] and as low as 200K in the presence of soluble salts [*Anderson and Tice*, 1989]. The possible formation of lenses and needles has important implications for water transport processes in the modern Martian climate. The presence of the light toned ice on Mars may indicate a higher degree of water mobility than previously suspected.

[33] Alternatively, frost can form in existing open cavities (larger than the soil pores), by vapor deposition on cold surfaces within the cavity, though it is difficult to envision a process by which such cavities might form at the landing site. Slow buckling of weakly cemented soils might occur as polygons deform over time. However, such deformation may take thousands of years and seasonal CO2 frost would load the surface more than 100 kg/m^2 of overburden and compress weakly supported cavities before ice had time to accumulate. Additionally, while initial ice condensation may form porous structures due to crystal growth being limited by diffusion of water vapor, over time continued condensation would fill these pores creating a solid ice mass, inconsistent with the observed structure of the light toned ice. On a smaller scale, *Fisher* [2005] proposed that microfractures caused by differential thermal contraction between pore ice and soil grains could create small openings in the pore ice. These openings might in turn allow additional ice condensation during the winter, where summer expansion would inflate the pore ice beyond the nominal soil porosity. While the details of such a process remain uncertain, the integrated accumulation of excess pore ice would potentially result in dense dark toned ice, different from the weak and light toned ice observed.

[34] Subaerial deposition and interannual accumulation of water frost or snow during a geologically recent climate cycle, in response to orbit oscillations, has been suggested to occur in some regions of Mars based on climate models [e.g., *Mischna et al.*, 2003; *Levrard et al.*, 2004]. To preserve the ice, subsequent burial by soil would need to be more rapid than the rate of climate change back to a state of unstable surface ice. Aeolian redistribution of soil could cover and preserve surface ice; however, there is no evidence of large scale movement of soil by wind at this location, and soil redistribution on this scale would potentially erase the polygonal ground. Additionally, light toned ice is found under two 5–6 cm scale partially buried rocks which were removed during excavation in Upper Cupboard and Ice Man. These rocks are too large to be emplaced by recent aeolian processes and their partial burial suggest they have been immobile for longer than ice has been stable at current depths [e.g., *Zent*, 2008].

[35] The heterogeneity of the ice deposits shows that there are strong heterogeneities in how ice forms in the subsurface and that different processes can operate in relative proximity to each other while experiencing the same climate history. Such heterogeneity implies other differences exist such as physical characteristics of the soil, soluble salts, surface geometry, etc. However, other observations from Phoenix do not indicate significant heterogeneity. OM observations show general homogeneity of soil grains in the bulk soil [*Pike et al.*, 2008]. Spectral analysis of surface and subsurface soils and ice do not indicate mineralogical differences that could be associated with salt mobility or local concentration [*Blaney et al.*, 2009]. Additionally, soluble salts appear homogeneously distributed [*Hecht et al.*, 2009; *Boynton et al.*, 2009]. Topographic variations are ubiquitous due to the trough and mound character of the polygonal ground, though light toned ice and ice-cemented soil both occur in the interior mound

region of two adjacent polygons. The ultimate cause of this heterogeneity remains a puzzle.

5. Summary and Conclusions

[36] Observations of ground ice from the Phoenix mission compare well with those from previous studies. Mars Odyssey observations from the Gamma Ray Spectrometer (GRS) and Neutron Spectrometer (NS) detected abundant ground ice widespread over the high latitudes of Mars [*Boynton et al.*, 2008; *Feldman et al.*, 2008], though at a low 450–600 km spatial resolution. Together with theoretical studies and analysis of seasonal brightness temperatures, prelanding predictions were that the ice table would be 2–6 cm below a layer of ice-free soil [*Mellon et al.*, 2008a]. Our mean ice table depth of 4.6 cm agrees remarkably well with these predictions. The Mars Odyssey data also indicates that ice exists in abundances of 75–80% by volume for the landing site region [*Feldman et al.*, 2008] which would exceed the pore volume of most soils. An areal mixture of the two types of ice observed at the landing site, ice-saturated soil and light toned ice, would require about 60% of the regional area to contain subsurface deposits of the light toned ice to yield an effective neutron count rate as seen by the NS in this region. The thickness of the light toned ice would not need to be more than a few cm to achieve this result, since ice exhibits a short mean free path for neutron energy exchange and would concentrate the neutrons within this layer [*Feldman et al.*, 1993] and the concentration of ice below a few cm into the ice is not sensed by the NS. Polygonal ground morphology, however, is sensitive to ice concentration (and resulting rheology) over greater depths and indicates the bulk of the subsurface consists of ice cemented soil [*Mellon et al.*, 2008b]. Since polygon ground develops over long periods (thousands of years or more) and requires the presence of shallow ground ice, it also indicates that the ice has been generally present for much longer than thousands of years. In regions equatorward of the Phoenix latitude small fresh impact craters have exposed ground ice in the upper meter of the permafrost, in some instances in concentrations similar to those of the light toned ice at the Phoenix site [*Byrne et al.*, 2009]. These observations suggest that the Phoenix landing site well represents the state of ice-rich permafrost on Mars.

[37] In summary, the subsurface distribution of high latitude ground ice was explored by the Phoenix spacecraft through a dozen trench complexes (and thruster pits) and for a range of polygon morphological provinces (polygon interiors, flanks, and troughs). Shallow ground ice was found to be abundant under a layer of relatively loose ice-free soil at the landing site, consistent with prelanding predictions. The mean depth of ground ice was found to be 4.6 cm, though not randomly sampled, but varies by more than 10x over the work space. These variations can be attributed mainly to slope effects and thermal inertia variations in the overburden soil affecting ground temperatures. The range of implied thermal inertia variations is consistent with a small degree of mineral cementing in loose soil. Combining the depth of the ice table, local slope, TECP thermal inertia, and surface albedo, the presence of ice is consistent with vapor-diffusive equilibrium with respect to a mean atmospheric water content of 3.4×10^{19} m^{-3} (consistent with an average summer time column abundance of 38 pr um), indicating that the current atmospheric water vapor abundance in the northern plains is representative of the conditions for the past 100–1000 yrs.

[38] Ice-cemented soil exposures dominate the subsurface, comprising about 90% of the icy material exposed by trenching, and are best explained as vapor deposited pore ice in a matrix supported porous soil. Ice cemented soil is believed to dominate the subsurface to depths of 10–15 m based on analysis of polygon geomorphology [*Mellon et al.*, 2008b, 2009]. Light toned ice deposits represent a minority of the subsurface (~10% of the excavated area) and are thought to represent relative thin near surface deposits. However, comparison with Mars Odyssey observations suggest this ice may be more common regionally than is represented by the sampling of Phoenix trenches. In areas not significantly altered by landing thrusters, this ice appears in diffusive equilibrium with the atmosphere. The relative purity of the light toned deposit is not consistent with vapor deposition in soil pores as with the ice-cemented soils. The formation of these relatively pure ice deposits appears most consistent with the formation of excess ice by soil ice segregation, such as would occur by thin film migration and the formation of ice lenses, needle ice, or similar ice structures.

[39] **Acknowledgments.** We wish to thank Phoenix team for their dedicated hard work that resulted in a safe landing and remarkably successful mission. Numerical modeling was supported in part by NASA grant NNX08AE33G. We would also like to thank Norbert Schorghofer and an anonymous reviewer for constructive reviews.

References

Aharonson, O., and N. Schorghofer (2006), Subsurface ice on Mars with rough topography, *J. Geophys. Res.*, *111*, E11007, doi:10.1029/2005JE002636.

Alexander, D. A., et al. (2006), Processing of Mars Exploration Rover imagery for science and operations planning, *J. Geophys. Res.*, *111*, E02S02, doi:10.1029/2005JE002462.

Anderson, D. M., and A. R. Tice (1972), Predicting unfrozen water contents in frozen soils from surface area measurements, *Highw. Res. Rec.*, *393*, 12–18.

Anderson, D. M., and A. R. Tice (1989), Unfrozen water contents of six Antarctic soil materials, in *Cold Regions Engineering: Proceedings of the Fifth International Conference*, edited by R. L. Michalowski, pp. 353–366, Am. Soc. of Civ. Eng., Reston, Va.

Arvidson, R. E., et al. (2009), Results from the Mars Phoenix Lander Robotic Arm experiment, *J. Geophys. Res.*, *114*, E00E02, doi:10.1029/2009JE003408.

Blaney, D. L., et al. (2009), Multi-spectral imaging of the Phoenix landing site: Characteristics of surface and subsurface ice, rocks, and soils, *Lunar Planet. Sci.*, *XL*, Abstract 2047.

Bonitz, R. G., et al. (2008), NASA Mars 2007 Phoenix Lander Robotic Arm and Icy Soil Acquisition Device, *J. Geophys. Res.*, *113*, E00A01, doi:10.1029/2007JE003030.

Boynton, W. V., G. J. Taylor, S. Karunatillake, R. C. Reedy, and J. M. Keller (2008), Elemental abundances determined via the Mars Odyssey GRS, in *The Martian Surface: Composition, Mineralogy, and Physical Properties*, edited by J. F. Bell, pp. 105–124, Cambridge U. Press, London.

Boynton, W. V., et al. (2009), Evidence for calcium carbonate at the Mars Phoenix landing site, *Science*, *325*, 61–64.

Byrne, S., et al. (2009), New impact craters probe buried Martian ice, *Science*, *325*, 1674–1676.

Chamberlain, M. A., and W. V. Boynton (2007), Response of Martian ground ice to orbit-induced climate change, *J. Geophys. Res.*, *112*, E06009, doi:10.1029/2006JE002801.

Fanale, F. P., J. R. Salvail, A. P. Zent, and S. E. Postawko (1986), Global distribution and migration of subsurface ice on Mars, *Icarus*, *67*, 1–18, doi:10.1016/0019-1035(86)90170-3.

Farmer, C. B., and P. E. Doms (1979), Global seasonal variations of water vapor on Mars and the implications for permafrost, *J. Geophys. Res.*, *84*, 2881–2888, doi:10.1029/JB084iB06p02881.

Feldman, W. C., W. V. Boynton, B. M. Jakosky, and M. T. Mellon (1993), Redistribution of subsurface neutrons caused by ground ice on Mars, *J. Geophys. Res.*, *98*, 20,855–20,870, doi:10.1029/93JE02325.

Feldman, W. C., M. T. Mellon, O. Gasnault, S. Maurice, and T. H. Prettyman (2008), Volatiles on Mars: Scientific results from the Mars Odyssey Neutron Spectrometer, in *The Martian Surface: Composition, Mineralogy, and Physical Properties*, edited by J. F. Bell, pp. 125–148, Cambridge Univ. Press, London.

Fisher, D. A. (2005), A process to make massive ice in the Martian regolith using long-term diffusion and thermal cracking, *Icarus*, *179*, 387–397, doi:10.1016/j.icarus.2005.07.024.

Hecht, M. H., et al. (2009), Detection of perchlorate and the soluble chemistry of Martian soil at the Phoenix Lander site, *Science*, *325*, 64–67.

Keller, H. U., et al. (2009), Physical properties of the icy soil at the Phoenix landing site, *Lunar Planet. Sci.*, *XL*, Abstract 1671.

Kossacki, K. J., and W. J. Markiewicz (2002), Martian Seasonal CO2 Ice in Polygonal Troughs in Southern Polar Region: Role of the Distribution of Subsurface H2O Ice, *Icarus*, *160*, 73–85, doi:10.1006/icar.2002.6936.

Kossacki, K. J., W. J. Markiewicz, and M. D. Smith (2003), Surface temperature of Martian regolith with polygonal features: Influence of the subsurface water ice, *Planet. Space Sci.*, *51*, 569–580, doi:10.1016/S0032-0633(03)00070-9.

Leighton, R. B., and B. C. Murray (1966), Behavior of carbon dioxide and other volatiles on Mars, *Science*, *153*, 136–144, doi:10.1126/science.153.3732.136.

Levrard, B., F. Forget, F. Montmssin, and J. Laskar (2004), Recent ice-rich deposits formed at high latitudes on Mars by sublimation of unstable equatorial ice during low obliquity, *Nature*, *431*, 1072–1075, doi:10.1038/nature03055.

Markiewicz, W. J., et al. (2009), Sublimation of exposed Snow Queen surface water ice as observed by the Phoenix Mars lander, *Lunar Planet. Sci.*, *XL*, Abstract 1667.

Mehta, M., N. O. Renno, M. R. Grover, and A. Sengupta (2008), Erosion dynamics during Phoenix landing on Mars, *Eos Trans. AGU*, *89*(53), Fall Meet. Suppl., Abstract U11B-0028.

Mellon, M. T., and B. M. Jakosky (1993), Geographic variations in the thermal and diffusive stability of ground ice on Mars, *J. Geophys. Res.*, *98*, 3345–3364, doi:10.1029/92JE02355.

Mellon, M. T., and B. M. Jakosky (1995), The distribution and behavior of Martian ground ice during past and present epochs, *J. Geophys. Res.*, *100*, 11,781–11,799, doi:10.1029/95JE01027.

Mellon, M. T., W. C. Feldman, and T. H. Prettyman (2004), The presence and stability of ground ice in the southern hemisphere of Mars, *Icarus*, *169*, 324–340, doi:10.1016/j.icarus.2003.10.022.

Mellon, M. T., W. V. Boynton, W. C. Feldman, R. E. Arvidson, T. N. Titus, J. L. Bandfield, N. E. Putzig, and H. G. Sizemore (2008a), A prelanding assessment of the ice table depth and ground ice characteristics in Martian permafrost at the Phoenix landing site, *J. Geophys. Res.*, *113*, E00A25, doi:10.1029/2007JE003067.

Mellon, M. T., R. E. Arvidson, J. J. Marlow, R. J. Phillips, and E. Asphaug (2008b), Periglacial landforms at the Phoenix landing site and the northern plains of Mars, *J. Geophys. Res.*, *113*, E00A23, doi:10.1029/2007JE003039.

Mellon, M. T., R. L. Fergason, and N. E. Putzig (2008c), The thermal inertia of the surface of Mars, in *The Martian Surface: Composition, Mineralogy, and Physical Properties*, edited by J. F. Bell, pp. 399–427, Cambridge Univ. Press, London.

Mellon, M. T., M. C. Malin, R. E. Arvidson, M. L. Searls, H. G. Sizemore, T. L. Heet, M. T. Lemmon, H. U. Keller, and J. Marshall (2009), The periglacial landscape at the Phoenix landing site, *J. Geophys. Res.*, doi:10.1029/2009JE003418, in press.

Miller, R. D. (1980), Freezing phenomena in soils, in *Applications in Soil Physics*, edited by D. Hillel, pp. 254–299, Academic, San Diego, Calif.

Miller, R. D., and P. B. Black (2003), Redistribution of water in terrestrial soils at subfreezing temperatures: A review of processes and their potential relevance to Mars, *J. Geophys. Res.*, *108*(E4), 8041, doi:10.1029/2002JE001873.

Mischna, M. A., M. I. Richardson, R. J. Wilson, and D. J. McCleese (2003), On the orbital forcing of Martian water and CO_2 cycles: A general circulation model study with simplified volatile schemes, *J. Geophys. Res.*, *108*(E6), 5062, doi:10.1029/2003JE002051.

Morris, R. V., M. T. Lemmon, R. E. Arvidson, D. L. Blaney, M. D. Ellehoj, and M. T. Mellon (2008), Time-dependent SSI multispectral properties for rock, soil, ice, and sublimation lags at the Phoenix landing site on Mars, *Eos Trans. AGU*, *89*(53), Fall Meet. Suppl., Abstract U11B-0029.

Paige, D. A. (1992), The thermal stability of near-surface ground ice on Mars, *Nature*, *356*, 43–45, doi:10.1038/356043a0.

Pike, W. T., U. Staufer, M. H. Hecht, and J. Marshall (2008), Microscopic investigation of Martian soil samples at the Phoenix site, *Eos Trans. AGU*, *89*(53), Fall Meet. Suppl., Abstract U14A-07.

Presley, M. A., and P. R. Christensen (1997), Thermal conductivity measurements of particulate materials. 2. Results, *J. Geophys. Res.*, *102*, 6551–6566, doi:10.1029/96JE03303.

Putzig, N. E., and M. T. Mellon (2007), Apparent thermal inertia and the surface heterogeneity of Mars, *Icarus*, *191*, 68–94, doi:10.1016/j.icarus.2007.05.013.

Shaw, A., R. E. Arvidson, R. Bonitz, J. Carsten, H. U. Keller, M. T. Lemmon, M. Mellon, M. Robinson, and A. Trebi-Ollennu (2009), Phoenix Soil Physical Properties Investigation, *J. Geophys. Res.*, doi:10.1029/2009JE003455, in press.

Sizemore, H. G., and M. T. Mellon (2006), Effects of soil heterogeneity on Martian ground-ice stability and orbital estimates of ice table depth, *Icarus*, *185*, 358–369, doi:10.1016/j.icarus.2006.07.018.

Sizemore, H. G., M. Mellon, M. Searls, M. T. Lemmon, A. P. Zent, T. L. Heet, R. E. Arvidson, D. L. Blaney, and H. U. Keller (2009), In situ analysis of ice table depth variations in the vicinity of small rocks at the Phoenix landing site, *J. Geophys. Res.*, doi:10.1029/2009JE003414, in press.

Smith, P. H., et al. (2008), Introduction to special section on the Phoenix Mission: Landing Site Characterization Experiments, Mission Overviews, and Expected Science, *J. Geophys. Res.*, *113*, E00A18, doi:10.1029/2008JE003083.

Smith, P. H., et al. (2009), H_2O at the Phoenix landing site, *Science*, *325*, 58–61.

Soons, J. M., and D. E. Greenland (1970), Observations of the growth of needle ice, *Water Resour. Res.*, *6*, 579–593, doi:10.1029/WR006i002p00579.

Taber, S. (1929), Frost heaving, *J. Geol*, *37*, 428–461, doi:10.1086/623637.

Titus, T. N., and T. H. Prettyman (2007), Thermal inertia characterization of the proposed Phoenix landing sites, *Lunar Planet. Sci.*, *XXXVIII*, Abstract 2088.

Washburn, A. L. (1980), *Geocryology: A Survey of Periglacial Processes and Environments*, John Wiley, New York.

Williams, P. J., and M. W. Smith (1989), *The Frozen Earth*, Cambridge Univ. Press, Cambridge, U. K.

Zent, A. P. (2008), A historical search for habitable ice at the Phoenix landing site, *Icarus*, *196*, 385–408, doi:10.1016/j.icarus.2007.12.028.

Zent, A. P., M. H. Hecht, D. R. Cobos, S. E. Wood, T. L. Hudson, S. M. Milkovich, L. P. DeFlores, and M. Mellon (2009), Initial results from the Thermal and Electrical Conductivity Probe (TECP) on Phoenix, *J. Geophys. Res.*, doi:10.1029/2009JE003420, in press.

R. E. Arvidson, S. Cull, and T. L. Heet, Department of Earth and Planetary Sciences, Washington University, Campus Box 1169, 1 Brookings Dr., Saint Louis, MO 63130-4862, USA.

D. L. Blaney and M. H. Hecht, Jet Propulsion Laboratory, 4800 Oak Grove Dr., Pasadena, CA 91109, USA.

H. U. Keller and W. J. Markiewicz, Max Planck Institute für Sonnensystemforschung, Max-Planck-Strasse 2, D-37191 Katlenburg-Lindau, Germany.

M. T. Lemmon, Department of Atmospheric Science, Texas A&M University, 3150 TAMU, College Station, TX 77843-3150, USA.

M. T. Mellon, M. L. Searls, and H. G. Sizemore, Laboratory for Atmospheric and Space Physics, University of Colorado at Boulder, Duane Physics Bldg., Campus Box 392, Boulder, CO 80309-0392, USA. (mellon@lasp.colorado.edu)

D. W. Ming and R. V. Morris, NASA Johnson Space Center, 2101 NASA Parkway, Houston, TX 77058, USA.

W. T. Pike, Electrical and Electronic Engineering, Imperial College of London, Exhibition Rd., London SW7 2AZ, UK.

A. P. Zent, Space Sciences Division, NASA Ames Research Center, MS 245-3, Moffett Field, CA 94035, USA.